

Substrate-Controlled Ultrafast Spin Injection and Demagnetization

J. K. Dewhurst,¹ S. Shallcross,² E. K. U. Gross,¹ and S. Sharma^{1,3,*}

¹Max-Planck Institut für Microstrukture Physics, Weinberg 2, D-06120 Halle, Germany

²Lehrstuhl für Theoretische Festkörperphysik, Staudtstr. 7-B2, 91058 Erlangen, Germany

³Max-Born Institute for Nonlinear Optics, Max-Born-Strasse 2A, 12489 Berlin, Germany

(Received 19 April 2018; revised manuscript received 12 June 2018; published 26 October 2018)

We investigate the laser-induced ultrafast injection of spin from a ferromagnetic (FM) material into a nonmagnetic (NM) one, for a diverse set of FM-NM interfaces. For all systems, we find the early time ($t < 20$ fs) spin dynamics to be driven by spin currents, with majority spin transferred to the NM and minority spin to the FM. At later times, spin-orbit-induced spin flips further demagnetize the FM, but also deplete the NM of the substantial spin moment injected during the sub-20-fs spin dynamics. We identify the density of unoccupied states in the NM material to be the key physical property that underpins the physics of ultrafast demagnetization of FM layers and a complex interplay of this density of states with the spin-orbit (SO) coupling strength of the NM substrate to be responsible for spin-injection efficiency.

DOI: 10.1103/PhysRevApplied.10.044065

I. INTRODUCTION

Ferromagnetic-nonmagnetic (FM-NM) interfaces represent the basic design architecture of both spin-injection as well as magnetic-memory devices [1]. As these represent crucial components of any future spintronics device [2–8], the laser-induced spin dynamics at FM-NM interfaces has been an intense topic of research [9–23]. It is widely believed that the spin-orbit (SO) coupling strength of the nonmagnetic layers plays a crucial role, controlling both the efficiency of spin injection across the interface as well as the amplitude and speed of demagnetization of the magnetic layers, which is significantly increased over the intrinsic demagnetization properties of the magnetic material [24–26]. However, the most important questions in this field, which guide our understanding of the underlying physics of these observations, remain unanswered: (a) Why does spin injection across the interface depend strongly on the SO coupling strength? (b) Are both, majority and minority, spin channels involved in the process of spin injection and demagnetization? (c) What underpins the enhanced amplitude of demagnetization found in the interface geometry? All these questions, if answered, would take us a step closer to the precise control of spins by light.

In the present work, we answer all these questions via fully *ab initio* calculation of laser-induced spin dynamics in the highly nonequilibrium state for several atomically clean interfaces: Co/Pt, Co/Au, Co/Al, Ni/Pt, Ni/Au, and Ni/Al. These extensive calculations reveal the existence of an early time ($t < 20$ fs) *spin-transfer phase* in which

optical excitation injects majority spins from the FM into the NM layers, while, simultaneously, minority-spin current flows into the FM layers. Subsequently, spin currents modulated by the SO interaction lead to spin-flip scattering, which causes an overall demagnetization of the multilayer. We find that the spin dynamics of both these phases are controlled to a large extent by the interface density of states, thus opening the way for the design of efficient spin-injection and magnetic-memory devices.

II. THEORY

The Runge-Gross theorem [27] establishes that the time-dependent external potential is a unique functional of the time-dependent density, given the initial state. Based on this theorem, a system of noninteracting particles can be chosen such that the density of this noninteracting system is equal to that of the interacting system for all times [28,29]. The wave function of this noninteracting system is represented as a Slater determinant of single-particle orbitals. In what follows, a fully noncollinear spin-dependent version of these theorems is employed [30]. The time-dependent Kohn-Sham (KS) orbitals are treated as Pauli spinors, which are determined by solving the following equations:

$$i \frac{\partial \psi_j(\mathbf{r}, t)}{\partial t} = \left[\frac{1}{2} \left(-i\nabla + \frac{1}{c} \mathbf{A}_{\text{ext}}(t) \right)^2 + v_s(\mathbf{r}, t) \right. \\ \left. + \frac{1}{2c} \boldsymbol{\sigma} \cdot \mathbf{B}_s(\mathbf{r}, t) + \frac{1}{4c^2} \boldsymbol{\sigma} \cdot [\nabla v_s(\mathbf{r}, t) \times -i\nabla] \right] \\ \times \psi_j(\mathbf{r}, t), \quad (1)$$

*sharma@mbi-berlin.de

where $\mathbf{A}_{\text{ext}}(t)$ is a vector potential representing the applied laser field and σ are the Pauli matrices. The KS effective potential $v_s(\mathbf{r}, t) = v_{\text{ext}}(\mathbf{r}, t) + v_H(\mathbf{r}, t) + v_{\text{XC}}(\mathbf{r}, t)$ is decomposed into the external potential v_{ext} , the classical electrostatic Hartree potential v_H , and the exchange-correlation (XC) potential v_{XC} . Similarly, the KS magnetic field is written as $\mathbf{B}_s(\mathbf{r}, t) = \mathbf{B}_{\text{ext}}(t) + \mathbf{B}_{\text{XC}}(\mathbf{r}, t)$, where $\mathbf{B}_{\text{ext}}(t)$ is the magnetic field of the applied laser pulse plus possibly an additional magnetic field and $\mathbf{B}_{\text{XC}}(\mathbf{r}, t)$ is the XC magnetic field. The final term of Eq. (1) is the spin-orbit coupling term. It is assumed that the wavelength of the applied laser is much greater than the size of a unit cell and the dipole approximation can be used, i.e., the spatial dependence of the vector potential is disregarded.

In order to analyze the contribution of each term in the Hamiltonian in Eq. (1) to the dynamics of the magnetization $\mathbf{M}(t) = \int \mathbf{m}(\mathbf{r}, t) d^3r = \int \langle \hat{\sigma} \hat{n}(\mathbf{r}, t) \rangle d^3r$, where \hat{n} is the density operator and $\mathbf{m}(\mathbf{r}, t)$ is the magnetization density, we start by calculating the dynamics of the magnetization density [31] using Ehrenfest's theorem:

$$\frac{\partial}{\partial t} m_j(\mathbf{r}, t) = i \langle [\hat{H}_s, \hat{\sigma}_j \hat{n}(\mathbf{r}, t)] \rangle. \quad (2)$$

Substitution of \hat{H}_s from Eq. (1) into Eq. (2) leads to

$$\begin{aligned} \frac{\partial}{\partial t} \mathbf{m}(\mathbf{r}, t) &= -\nabla \cdot \overleftrightarrow{\mathbf{J}}(\mathbf{r}, t) + \frac{1}{c} [\mathbf{B}_s(\mathbf{r}, t) \times \mathbf{m}(\mathbf{r}, t)] \\ &\quad + \frac{1}{4c^2} [\nabla n(\mathbf{r}, t) \times \nabla v_S(\mathbf{r}, t)] \\ &\quad + \frac{1}{2c^2} [\overleftrightarrow{\mathbf{J}}^T(\mathbf{r}, t) - \text{Tr}\{\overleftrightarrow{\mathbf{J}}(\mathbf{r}, t)\}] \\ &\quad \cdot \nabla v_S(\mathbf{r}, t), \end{aligned} \quad (3)$$

where $\overleftrightarrow{\mathbf{J}}(\mathbf{r}) = \overleftrightarrow{\mathbf{J}}_p(\mathbf{r}) + \overleftrightarrow{\mathbf{J}}_d(\mathbf{r})$ corresponds to the total spin-current tensor with paramagnetic component $\overleftrightarrow{\mathbf{J}}_p(\mathbf{r}) = \langle \hat{\sigma} \otimes (1/2)\{\hat{n}(\mathbf{r}), \hat{\mathbf{p}}\} \rangle$ and diamagnetic component $\overleftrightarrow{\mathbf{J}}_d(\mathbf{r}) = \mathbf{m}(\mathbf{r}) \otimes (1/c)\mathbf{A}_{\text{ext}}$.

The first term in Eq. (3) integrates to zero [31], i.e., it does not contribute to the global change in moment. However, this term dominates the physics of local moment change due to the flow of the spin current from one part of the material to another [32], e.g., from ferromagnetic to nonmagnetic layers in the present work. In all calculations, we use the adiabatic local-spin-density approximation (ALSDA) [33], which implies that the second term of Eq. (3), $\mathbf{B}_s(\mathbf{r}, t) \times \mathbf{m}(\mathbf{r}, t)$, is identically zero at each point in space and time [34]. In a recent work, it was demonstrated that this limitation does not significantly affect spin dynamics in interfaces [35,36], where magnetic anisotropy energy is of the order of a few milli-electron-volts. The third term of Eq. (3) also integrates to zero. The final term in Eq. (3) shows the interplay of the SO coupling and the spin currents.

III. COMPUTATIONAL DETAILS

All implementations employ the state-of-the art full-potential linearized augmented plane wave (LAPW) method. Within this method, the core electrons (with eigenvalues 95 eV below the Fermi energy) are treated fully relativistically by solving the radial Dirac equation, while higher-lying electrons are treated using the scalar relativistic Hamiltonian in the presence of the spin-orbit coupling. To obtain the two-component Pauli spinor states, the Hamiltonian containing only the scalar potential is diagonalized in the LAPW basis: this is the first variational step. The scalar states thus obtained are then used as a basis to set up a second-variational Hamiltonian with spinor degrees of freedom [37]. This is more efficient than simply using spinor LAPW functions; however, care must be taken to ensure that a sufficient number of first-variational eigenstates are used to ensure convergence of the second-variational problem.

A fully noncollinear version of time-dependent density functional theory as implemented within the ELK code [38] is used for all calculations [39]. A regular mesh in \mathbf{k} -space of $8 \times 8 \times 1$ is used and a time step of $\Delta t = 0.002$ fs is employed for the time-propagation algorithm [40]. A smearing width of 0.027 eV is used. For all ground-state calculations, a full structural optimization is performed. We find that the effects of lattice relaxation are very small in the spin dynamics in these interfaces. For all the cases, three layers of magnetic metal (Co or Ni) form an interface with five layers of nonmagnetic metal. Three kinds of nonmagnetic metals are used: Al, Au, and Pt. The (001) plane of the nonmagnetic metal is used. The interfaces are atomically clean and we assume that no alloying occurs at the interface. This is an important assumption, as the results for alloyed, rough, and/or dirty interfaces differ from the present data.

We solve Eq. (1) for the electronic system alone. Coupling of the electronic system to the nuclear degrees of freedom is not included in the present work. Radiative effects, which can be included by simultaneously time-propagating Maxwell's equations, are also not included in the present work. At longer time scales, these effects are expected to contribute significantly.

IV. RESULTS

In Fig. 1 are shown results for magnetization dynamics as a function of time for three monolayers (MLs) of Co and three MLs of Ni on various nonmagnetic metals. We first examine the spin dynamics of the magnetic layers, displayed as the normalized moment for three MLs of Co [Fig. 1(a)] and for three MLs of Ni [Fig. 1(b)]. These magnetic layers all demagnetize significantly upon excitation with the linearly polarized laser pump pulse; we employ a pulse with full width at half maximum (FWHM) 12 fs, frequency $\omega = 1.55$ eV, and a fluence of $E = 29$ mJ/cm².

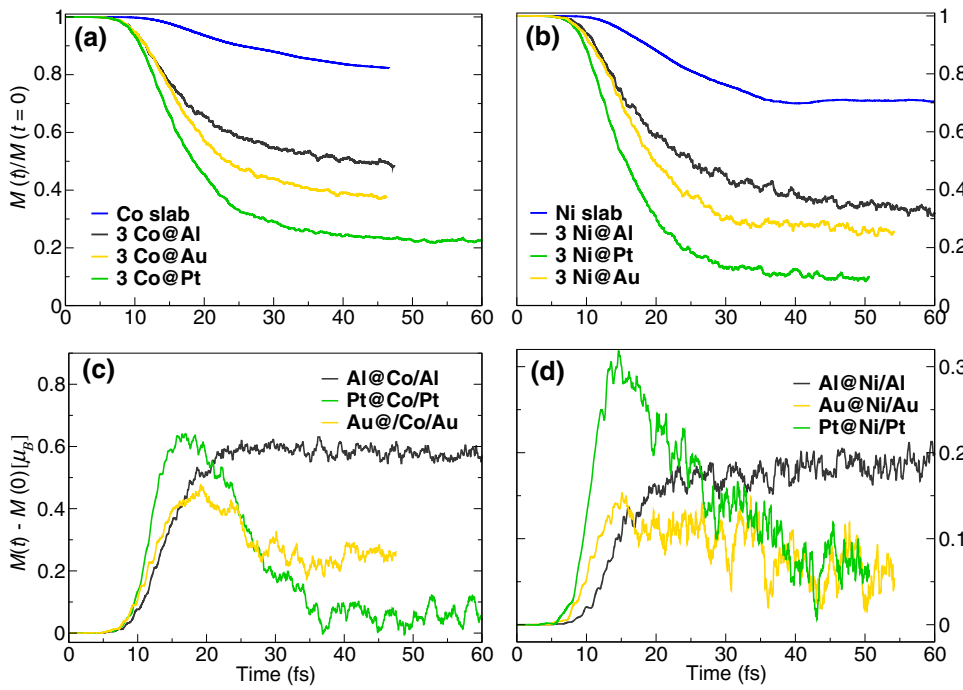


FIG. 1. The normalized moment [$M(t)/M(t = 0)$] as a function of time (in fs) for (a) three layers of Co and (b) three layers of Ni on various nonmagnetic metals. The change in the moment, $M(t) - M(t = 0)$ (in μ_B), as a function of time for the nonmagnetic layers in (c) a Co-NM interface and (d) a Ni-NM interface.

The amplitude of this demagnetization in FM layers is, however, seen to be profoundly sensitive to the type of nonmagnetic metal at the interface, with minimum demagnetization observed for FM-Al(001) and the maximum for FM-Pt(001). On comparing the demagnetization of these interfaces with the slab of FM material deposited on an insulating substrate [see Figs. 1(a) and 1(b)], we note that the amplitude of demagnetization is greatly enhanced in the interface as compared to the slab. In the past, a similar enhancement in the amplitude and speed of demagnetization of a Co/Pt(001) interface as compared to a Co slab has been experimentally demonstrated, and it was concluded that the SO coupling of Pt, which is much larger than that of Co, underpinned this observed increase in the amplitude of demagnetization [24,25,41]. In the present work as well, we see that on going from Al to Pt as the SO coupling constant increases, the amplitude of demagnetization also increases. It is also interesting to note that the rate of demagnetization for $t > 35$ fs is the same ($0.006 \mu_B/\text{fs}$ for Co-NM and $0.005 \mu_B/\text{fs}$ for Ni-NM) for all interfaces and that the SO coupling constant of the nonmagnetic metal plays no role in this time regime. However, it is important to mention that since the Elliot-Yaffet-like scattering [14,42–44] due to impurities and phonons is not included in the present work, this rate is expected to be underestimated for longer times (of the order of 100 fs).

We now turn our attention to the spin dynamics in the nonmagnetic layers of the interface: these results are shown for Co-NM in Fig. 1(c) and for Ni-NM in Fig. 1(d). The moment of the nonmagnetic layers shows an initial increase (for times ≤ 25 fs). The amplitude of this increase

in moment [45] is a maximum for Pt and a minimum for Au substrate. The subsequent demagnetization in the Pt and Au layers is large and almost all the induced moment is lost. In contrast to this, the Al layers remain in a transient magnetic state until the end of our simulation at 100 fs. It is important to mention that in case of FM-Pt(001), the induced moment on the Pt layers is lost within about 25 fs, making it experimentally challenging to observe. These findings raise the question of whether the increase in the amplitude of demagnetization can, beyond the apparent trend of the results, be definitively tied to the SO coupling constant. We will now explore this question.

The key difference between the slab and the interface geometry is that in the latter case spin current is allowed to flow across the interface. To understand what percentage of the total demagnetization in the magnetic layers is due to the flow of spin current [32], we compare the total spin dynamics with a simulation in which the SO interaction is switched off. In this case, the equation of motion involves only the divergence of the total current tensor [see Eq. (3)] and thus demagnetization can only occur due to spin transfer, as spin-flip processes are not allowed. The total spin moment of the material is then conserved, i.e., the sum of the following three stays constant in time: (i) the moment of the magnetic layers, (ii) the moment gained by the nonmagnetic substrate layers, and (iii) the moment of the highly excited electrons that cannot be assigned to any of the atoms. The magnetic moments of the Co and NM layers, obtained in the absence of SO coupling, in Co-NM interfaces are shown in Fig. 2 (the contribution from highly excited electrons is not shown in this figure).

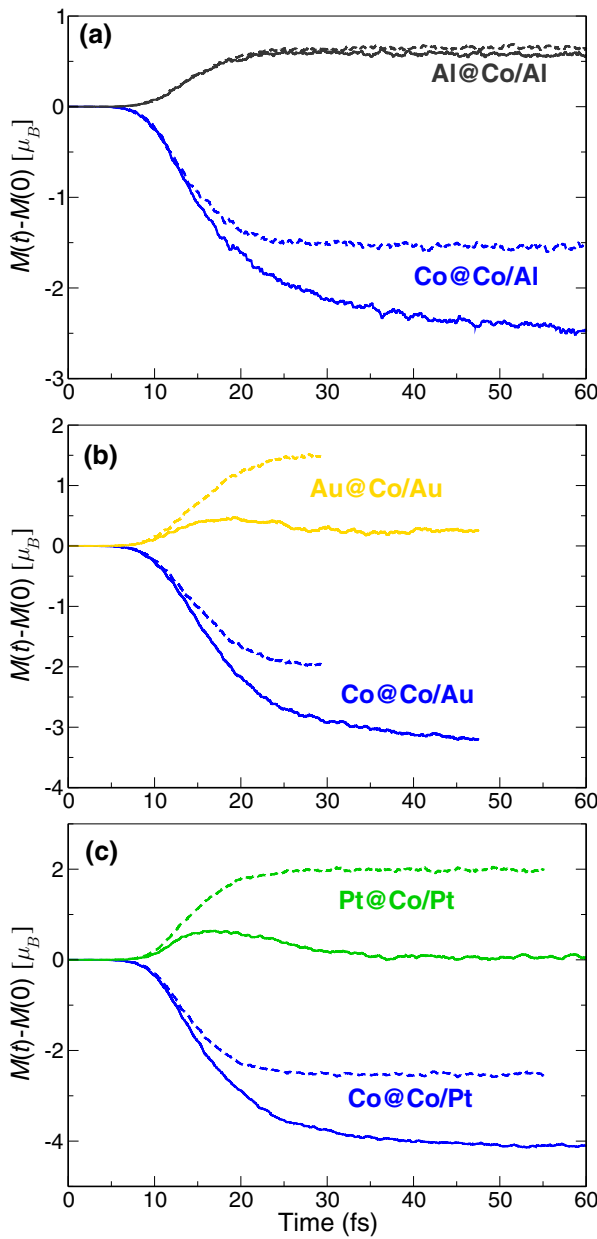


FIG. 2. The change in moment, $M(t) - M(t = 0)$ (in μ_B), as a function of time (in fs) calculated with (solid lines) and without SO coupling (dashed lines). The results are shown for (a) $\text{Co/Al}(001)$, (b) $\text{Co/Au}(001)$, and (c) $\text{Co/Pt}(001)$.

It is clear from these data that the demagnetization dynamics can be divided into *three time scales*:

(1) Below 20 fs, the purely spin-current-induced demagnetization of the Co layers is almost the same as the total demagnetization, i.e., the moment loss in the magnetic layers is dominated by spin transfer from the magnetic to the nonmagnetic layers. This spin transfer also results in an increase of the moment on the nonmagnetic layers. The early time spin dynamics of the Co-NM interface is thus dominated by the optically

induced intersite spin transfer (OISTR) physics [46], found previously to dominate the early time spin dynamics of magnetic FM-antiferromagnetic(-AFM) multilayers and the Heusler alloys [47]. During this time (below 20 fs), the demagnetization rate is slowest for FM-Al ($0.15 \mu_B/\text{fs}$ for $\text{Co/Al}(001)$ and $0.05 \mu_B/\text{fs}$ for $\text{Ni/Al}(001)$) and fastest for FM-Pt ($0.27 \mu_B/\text{fs}$ for $\text{Co/Pt}(001)$ and $0.12 \mu_B/\text{fs}$ for $\text{Ni/Pt}(001)$).

(2) After about 20 fs, in the absence of SO, the demagnetization curve saturates; however, with SO switched on, further significant demagnetization is seen between 20 and 35 fs. In this time window, both spin flips and spin currents together are involved in the spin dynamics [again see Eq. (3)] and, as a consequence, demagnetization of both the Co and the nonmagnetic layers occurs.

(3) For times greater than 35 fs, spin flips alone dominate the demagnetization. During this period, the SO coupling of the nonmagnetic metal does not influence the spin dynamics of the magnetic layers and the Co layers in all interfaces demagnetize at the same rate (same trend is seen in the Ni-NM interfaces).

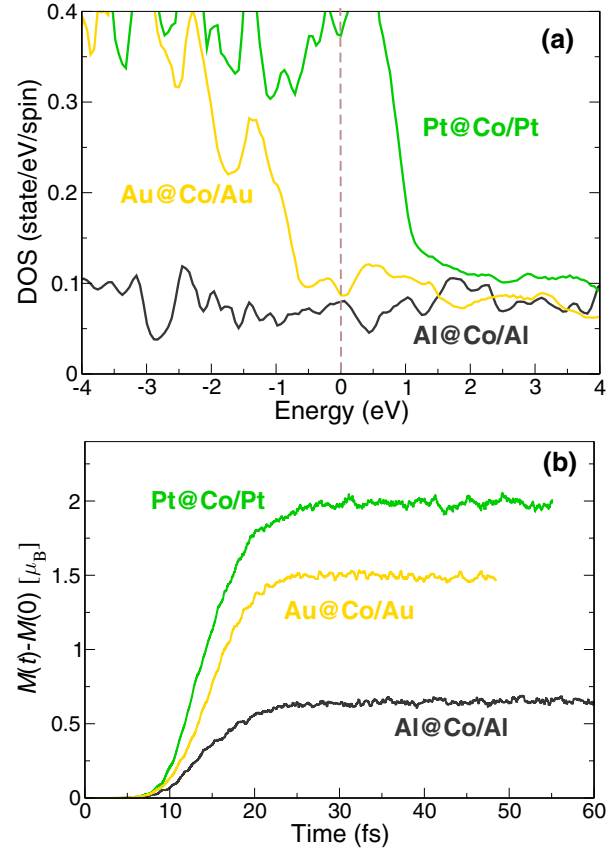


FIG. 3. (a) The ground-state density of states (in states per electron volt per spin) projected on the interface nonmagnetic layer. (b) The change in moment (in μ_B) as a function of time (in fs) for the nonmagnetic layers. This change in moment is calculated without a SO coupling term in the Hamiltonian.

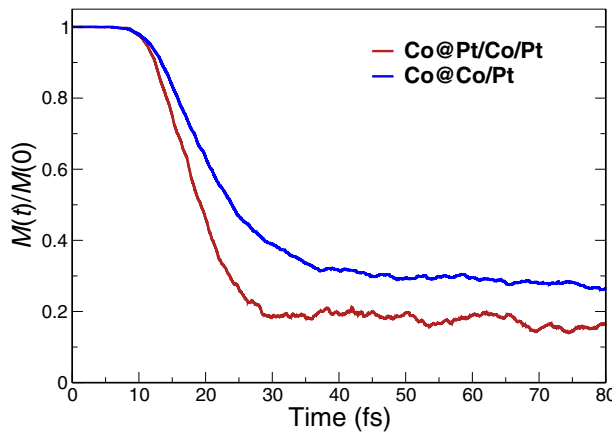


FIG. 4. The normalized moment as a function of time (in fs) for Co layers in Co/Pt(001) (red) and Pt(001)/Co/Pt(001) (blue).

These three time scales in the demagnetization process have been confirmed experimentally [48] for Co/Cu(001). Thus, despite the apparent trend that the demagnetization amplitude increases with increasing SO, the present results show that the amplitude of this demagnetization is dominated by OISTR (i.e., spin currents) [46]. A closer look shows that the contribution of OISTR to the amplitude of total demagnetization is approximately 78% in Co/Al and about 60% in Co/Pt, making it the most significant term in the early time spin dynamics of FM-NM interfaces.

It still remains to be understood as to why the spin current (and hence the amplitude of demagnetization) increases on going from Al to Pt. To understand this,

we examine the density of states (DOS) of the Al, Au, and Pt layers at the interface. In Fig. 3(a) is shown the interface-layer projected DOS and in Fig. 3(b) the comparison of the moment in these layers (Al, Au, and Pt) as a function of time and in the absence of SO coupling. The number of available states (above the Fermi level) is a maximum for Pt and a minimum for Al in the energy range 0–1.55 eV, which is the frequency of the pump laser pulse. The current-induced magnetic moment in these nonmagnetic layers shows exactly the same trend, implying that the availability of states plays a major role in the early time increase in amplitude of demagnetization on going from Al to Pt and not, as previously assumed, the increase in the SO coupling constant.

These results are interesting in that given the high fluence of the laser pulse, the dynamics is expected to be highly nonlinear, yet we find that the ground-state DOS gives an indication of the observed early time spin dynamics. Similar physics has been observed in both FM-AFM interfaces [46], as well as in the Heusler alloys [47], and the underlying reason for this is that the linear-order term in the current is very important, and hence OISTR is largely decided by the ground-state DOS.

These results suggest that if one were to make an interface of the kind NM-FM-NM, such that the current could flow from the FM layers across both interfaces, then this should lead to a further increase in the amplitude of demagnetization of the FM layers. In order to test this, we perform such calculations for Pt(001)/Co/Pt(001) and the results, together with those of Co/Pt(001), are presented in Fig. 4. As expected, the amplitude of demagnetization is enhanced in a Pt-rich interface. Furthermore, this

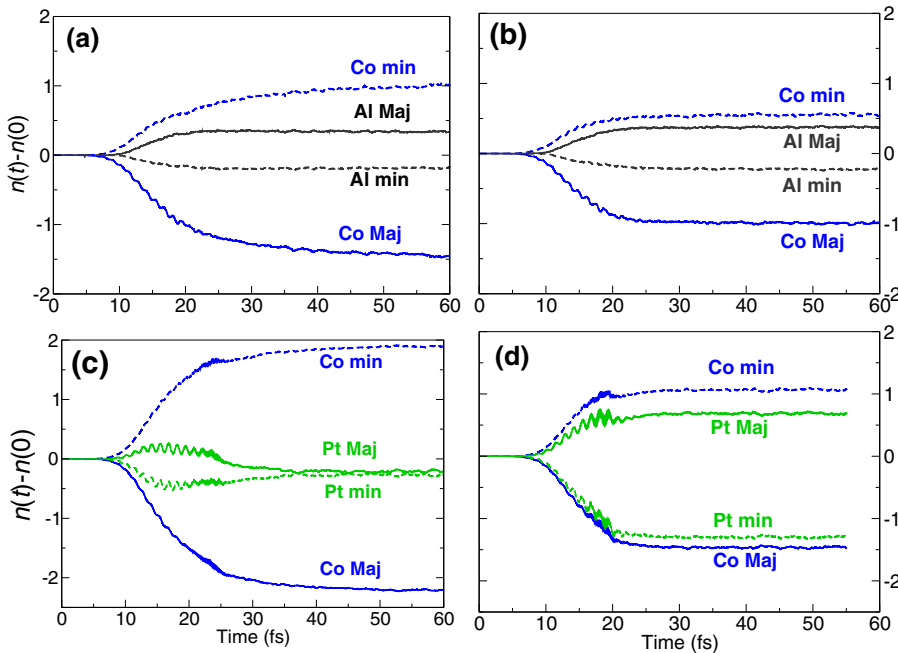


FIG. 5. The number of majority (Maj) and minority (min) electrons as a function of time (in fs). The results calculated with the full Hamiltonian are presented for (a) Co/Al(001) and (c) Co/Pt(001). The results calculated in the absence of SO coupling are presented for (b) Co/Al(001) and (d) Co/Pt(001).

enhancement takes place in the spin-current dominated time scale of < 20 fs, indicating an increase in OISTR across the interface to be the main reason for this amplitude enhancement.

To understand the nature of the spin currents in these systems, we now examine the time dependence of the number of majority and minority electrons in the magnetic and nonmagnetic layers. Such results for Co/Al(001) and Co/Pt(001) are shown in Fig. 5. We first consider the results obtained without SO coupling [panels (b) and (d) of Fig. 5]. With SO coupling switched off, demagnetization of magnetic layers occurs only due to intersite spin transfer (i.e., the flow of spin current across the interface), visible from these results through the approximate compensation of the decrease of in majority-spin electrons in the Co layers and a corresponding increase in the Al and Pt layers (leading to the observed increase in the moment on these nonmagnetic layers). Interestingly, we also find that a large number of minority carriers also move from the nonmagnetic layers to the Co layers, apparent as an increase in the minority carriers of the Co layers and a corresponding decrease in the Al and Pt layers. This enhances the amplitude of both the demagnetization of the magnetic layers and the magnetization of the nonmagnetic layers. The total spin-up and spin-down occupation numbers are not strictly conserved because some of the electrons are excited into high-energy states that are highly delocalized and hence cannot be associated with either the magnetic or nonmagnetic atoms.

We now consider the corresponding results when the SO coupling is included. The presence of SO coupling leads to spin flips in the Al and Pt layers, thereby increasing the number of minority carriers and decreasing the number of majority carriers in these layers. These minority carriers can also then flow into the Co layers, leading to further demagnetization of the Co layers. These spin flips from the majority- to the minority-spin channel in Al and Pt layers also have the effect of providing more empty majority states in these layers, and thus more majority electrons can flow from Co into these empty majority states. This then further enhances the amplitude of demagnetization of Co. These results clearly indicate that the mechanism of demagnetization involves spin currents of both minority and majority states, and is not dominated by a flow of majority carriers into the nonmagnetic layers, as proposed by the superdiffusive model [49–51]. In fact, the total demagnetization is due equally to an injection of minority-spin carriers into and a flow of majority-spin carriers out of magnetic layers. At this point, it is important to mention that when the material demagnetizes, we do not see any increase in the orbital angular moment. Hence we expect that the moment goes to the lattice at subfemtosecond time scales, leading to the conservation of global angular momentum.

TABLE I. The spin-injection efficiency (in %) calculated in two different ways: the second column is calculated based on total moment (see the text for details) and the third column is based on the number of majority carriers (see the text for details).

Interface	Efficiency (a)	Efficiency (b)
Co/Al(001)	41	30
Co/Au(001)	12	22
Co/Pt(001)	19	8
Ni/Al(001)	20	26
Ni/Au(001)	29	6
Ni/Pt(001)	32	4

For spintronic devices based on FM-NM interfaces, it is crucial to have a large spin-injection efficiency [26], i.e., the percentage of majority spins lost by the magnetic layer that is gained by the nonmagnetic layers should be high. This efficiency can be defined in two ways involving changes of either the magnetic moment in the FM and NM layers or changes in the number of majority electrons in these layers: i.e., as either $\Delta M_{\text{NM}}(t)/\Delta M_{\text{FM}}(t)$, where ΔM_{FM} is the loss in moment of the FM layers and ΔM_{NM} is the gain in moment on the nonmagnetic layers or $\Delta n_{\text{NM}}(t)/\Delta n_{\text{FM}}(t)$, where Δn_{FM} is the loss in majority carriers of the FM layers and Δn_{NM} is the gain in the majority carriers by the nonmagnetic layers. As we demonstrate in Fig. 5, both spin channels play a significant role in changing of the moment of the NM layers, and hence the second of these definitions is the more rigorous, although it is more difficult to use experimentally. Thus we now calculate the spin-injection efficiency for all FM-NM interfaces using both these definitions (see Table I) at $t = 20$ fs. From these results, it is clear that by either definition, Co/Al(001) has the highest spin-injection efficiency.

V. CONCLUSIONS

Through the employment of a fully *ab initio* description of laser-induced nonequilibrium spin dynamics in conjunction with an extensive set of ferromagnetic-nonmagnetic interfaces, we study the ultrafast demagnetization of the ferromagnetic (FM) layers, and spin injection into the nonmagnetic (NM) layers. Our key finding is that the initial spin dynamics ($t < \sim 20$ fs) is driven almost entirely by optically induced spin transfer across the interface, controlled by the availability of unoccupied states. Both spin channels are equally active in this *spin-transfer phase*, which involves the flow of majority-spin states into the NM layers and, at the same time, minority-spin states into the FM layers. This results in demagnetization of the FM layers and a simultaneous substantial magnetization of the NM layers, with little change in the total system moment. After this all-optical phase, majority- and minority-spin currents couple via the spin-orbit (SO) interaction, resulting in further demagnetization of the FM layers and, in

the case of strong spin-orbit coupling, almost complete demagnetization of the NM layers. For longer times, spin currents play no role and the subsequent slow depolarization rate is driven by spin-flip scattering induced by the electron-electron interaction as well as the Elliot-Yaffet mechanism. We thus identify the density of available states and the spin-orbit coupling in the nonmagnetic material as two key parameters controlling both ultrafast demagnetization as well as spin injection into the NM. To optimize ultrafast demagnetization, both of these should be maximized, while for spin-injection efficiency their interplay is more complex—on the one hand, SO-mediated spin flips, from majority to minority, make more majority states available for spin injection, while on the other, such spin flips reduce the majority-spin-injection efficiency.

ACKNOWLEDGMENTS

Sharma would like to thank DFG for funding through TRR227 and SPP-QUTIF.

-
- [1] C.-H. Lambert, S. Mangin, B. S. Varaprasad, Y. K. Takahashi, M. Hehn, M. Cinchetti, G. Malinowski, K. Hono, Y. Fainman, M. Aeschlimann, and E. E. Fullerton, All-optical control of ferromagnetic thin films and nanostructures, *Science* **345**, 1337 (2014).
 - [2] S. A. Wolf, D. D. Awschalom, R. A. Buhrman, J. M. Daughton, S. von Molnár, M. L. Roukes, A. Y. Chtchelkina, and D. M. Treger, Spintronics: A spin-based electronics vision for the future, *Science* **294**, 1488 (2001).
 - [3] S. M. Falke, C. A. Rozzi, D. Brida, M. Maiuri, M. Amato, E. Sommer, A. De Sio, A. Rubio, G. Cerullo, E. Molinari, and C. Lienau, Coherent ultrafast charge transfer in an organic photovoltaic blend, *Science* **344**, 1001 (2014).
 - [4] T. Graf, C. Felser, and S. Parkin, Heusler compounds: in *Handbook of Spintronics*, edited by Y. Xu, D. D. Awschalom, and J. Nitta (Springer, Dordrecht, 2016), Chap. 9, p. 335.
 - [5] A. Melnikov, I. Razdolski, T. O. Wehling, E. T. Papaioannou, V. Roddatis, P. Fumagalli, O. Aktsipetrov, A. I. Lichtenstein, and U. Bovensiepen, Ultrafast Transport of Laser-Excited Spin-Polarized Carriers in Au/Fe/MgO(001), *Phys. Rev. Lett.* **107**, 076601 (2011).
 - [6] M. Cinchetti, K. Heimer, J.-P. Wuestenberg, O. Andreyev, M. Bauer, S. Lach, C. Ziegler, Y. Gao, and M. Aeschlimann, Determination of spin injection and transport in a ferromagnet/organic semiconductor heterojunction by two-photon photoemission, *Nat. Mater.* **8**, 115 (2009).
 - [7] A. Alekhin, I. Razdolski, N. Ilin, J. P. Meyburg, D. Diesing, V. Roddatis, I. Rungger, M. Stamenova, S. Sanvito, U. Bovensiepen, and A. Melnikov, Femtosecond Spin Current Pulses Generated by the Nonthermal Spin-Dependent Seebeck Effect and Interacting with Ferromagnets in Spin Valves, *Phys. Rev. Lett.* **119**, 017202 (2017).
 - [8] I. Razdolski, A. Alekhin, N. Ilin, J. P. Meyburg, V. Roddatis, D. Diesing, U. Bovensiepen, and A. Melnikov, Nanoscale interface confinement of ultrafast spin transfer torque driving non-uniform spin dynamics, *Nat. Commun.* **8**, 15007 (2017).
 - [9] U. Bovensiepen, Femtomagnetism: Magnetism in step with light, *Nat. Phys.* **5**, 461 (2009).
 - [10] L. Guidoni, E. Beaurepaire, and J.-Y. Bigot, Magneto-Optics in the Ultrafast Regime: Thermalization of Spin Populations in Ferromagnetic Films, *Phys. Rev. Lett.* **89**, 017401 (2002).
 - [11] J.-Y. Bigot, M. Vomir, and E. Beaurepaire, Coherent ultrafast magnetism induced by femtosecond laser pulses, *Nat. Phys.* **5**, 515 (2009).
 - [12] C. Stamm, T. Kachel, N. Pontius, R. Mitzner, T. Quast, K. Holldack, S. Khan, C. Lupulescu, E. F. Aziz, M. Wietstruk, H. A. Durr, and W. Eberhardt, Femtosecond modification of electron localization and transfer of angular momentum in nickel, *Nat. Mater.* **6**, 740 (2007).
 - [13] A. Eschenlohr, M. Battiato, P. Maldonado, N. Pontius, T. Kachel, K. Holldack, R. Mitzner, A. Föhlisch, P. M. Oppeneer, and C. Stamm, Ultrafast spin transport as key to femtosecond demagnetization, *Nat. Mater.* **12**, 332 (2013).
 - [14] E. Turgut, C. La-o vorakiat, J. M. Shaw, P. Grychtol, H. T. Nembach, D. Rudolf, R. Adam, M. Aeschlimann, C. M. Schneider, T. J. Silva, M. M. Murnane, H. C. Kapteyn, and S. Mathias, Controlling the Competition Between Optically Induced Ultrafast Spin-Flip Scattering and Spin Transport in Magnetic Multilayers, *Phys. Rev. Lett.* **110**, 197201 (2013).
 - [15] S. Essert and H. Schneider, Electron-phonon scattering dynamics in ferromagnetic metals and their influence on ultrafast demagnetization processes, *Phys. Rev. B* **84**, 224405 (2011).
 - [16] C. Illg, M. Haag, and M. Fähnle, Ultrafast demagnetization after laser irradiation in transition metals: *Ab initio* calculations of the spin-flip electron-phonon scattering with reduced exchange splitting, *Phys. Rev. B* **88**, 214404 (2013).
 - [17] M. Krau, T. Roth, S. Alebrand, D. Steil, M. Cinchetti, M. Aeschlimann, and H. C. Schneider, Ultrafast demagnetization of ferromagnetic transition metals: The role of the Coulomb interaction, *Phys. Rev. B* **80**, 180407 (2009).
 - [18] A. B. Schmidt, M. Pickel, M. Donath, P. Buczek, A. Ernst, V. P. Zhukov, P. M. Echenique, L. M. Sandratskii, E. V. Chulkov, and M. Weinelt, Ultrafast Magnon Generation in an Fe Film on Cu(100), *Phys. Rev. Lett.* **105**, 197401 (2010).
 - [19] C. Andrea Rozzi, S. Maria Falke, N. Spallanzani, A. Rubio, E. Molinari, D. Brida, M. Maiuri, G. Cerullo, H. Schramm, J. Christoffers, and C. Lienau, Quantum coherence controls the charge separation in a prototypical artificial light-harvesting system, *Nat. Commun.* **4**, 1602 (2013).
 - [20] A. B. Schmidt, M. Pickel, M. Wiemhöfer, M. Donath, and M. Weinelt, Spin-Dependent Electron Dynamics in Front of a Ferromagnetic Surface, *Phys. Rev. Lett.* **95**, 107402 (2005).
 - [21] T. Kampfrath, M. Battiato, P. Maldonado, G. Eilers, J. Nötzold, S. Märlein, V. Zbarsky, F. Freimuth, Y. Mokrousov, S. Blügel, M. Wolf, I. Radu, P. M. Oppeneer, and M. Münenberg, Terahertz spin current pulses controlled by magnetic heterostructures, *Nat. Nanotechnol.* **8**, 256 (2013).

- [22] A. Kirilyuk, A. V. Kimel, and T. Rasing, Ultrafast optical manipulation of magnetic order, *Rev. Mod. Phys.* **82**, 2731 (2010).
- [23] J. Simoni, M. Stamenova, and S. Sanvito, *Ab initio* dynamical exchange interactions in frustrated antiferromagnets, *Phys. Rev. B* **96**, 054411 (2017).
- [24] C. v.-K. Schmising, M. Giovannella, D. Weder, S. Schafert, J. Webb, and S. Eisebitt, Nonlocal ultrafast demagnetization dynamics of Co/Pt multilayers by optical field enhancement, *New J. Phys.* **17**, 033047 (2015).
- [25] K. C. Kuiper, T. Roth, A. J. Schellekens, O. Schmitt, B. Koopmans, M. Cinchetti, and M. Aeschlimann, Spin-orbit enhanced demagnetization rate in Co/Pt-multilayers, *Appl. Phys. Lett.* **105**, 202402 (2014).
- [26] M. Hofherr, P. Maldonado, O. Schmitt, M. Berrieta, U. Bierbrauer, S. Sadashivaiah, A. J. Schellekens, B. Koopmans, D. Steil, M. Cinchetti, B. Stadtmüller, P. M. Oppeneer, S. Mathias, and M. Aeschlimann, Speed and efficiency of femtosecond spin current injection into a nonmagnetic material, *Phys. Rev. B* **96**, 100403 (2017).
- [27] E. Runge and E. Gross, Density Functional Theory for Time-Dependent Systems, *Phys. Rev. Lett.* **52**, 997 (1984).
- [28] C. A. Ullrich, *Time-Dependent Density-Functional Theory Concepts and Applications* (Oxford University Press, Oxford, New York, 2011).
- [29] S. Sharma, J. K. Dewhurst, and E. K. U. Gross, *Optical Response of Extended Systems Using Time-Dependent Density Functional Theory* (Springer, Berlin, Heidelberg, 2014), p. 235.
- [30] K. Krieger, J. K. Dewhurst, P. Elliott, S. Sharma, and E. K. U. Gross, Laser-induced demagnetization at ultrashort time scales: Predictions of TDDFT, *J. Chem. Theory Comput.* **11**, 4870 (2015).
- [31] K. Krieger, P. Elliott, T. Müller, N. Singh, J. K. Dewhurst, E. K. U. Gross, and S. Sharma, Ultrafast demagnetization in bulk versus thin films: An *ab initio* study, *J. Phys.: Condens. Matter* **29**, 224001 (2017).
- [32] V. Shokeen, M. Sanchez Piaia, J.-Y. Bigot, T. Müller, P. Elliott, J. K. Dewhurst, S. Sharma, and E. K. U. Gross, Spin Flips Versus Spin Transport in Nonthermal Electrons Excited by Ultrashort Optical Pulses in Transition Metals, *Phys. Rev. Lett.* **119**, 107203 (2017).
- [33] U. von Barth and L. Hedin, A local exchange-correlation potential for the spin polarized case, *J. Phys. C: Solid State Phys.* **5**, 1629 (1972).
- [34] S. Sharma, J. K. Dewhurst, C. Ambrosch-Draxl, S. Kurth, N. Helbig, S. Pittalis, S. Shallcross, L. Nordström, and E. K. U. Gross, First-Principles Approach to Noncollinear Magnetism: Towards Spin Dynamics, *Phys. Rev. Lett.* **98**, 196405 (2007).
- [35] J. K. Dewhurst, A. Sanna, and S. Sharma, Effect of exchange-correlation spin-torque on spin dynamics, *Eur. Phys. J. B* **91**, 218 (2018).
- [36] S. Sharma, E. K. U. Gross, A. Sanna, and J. K. Dewhurst, Source-free exchange-correlation magnetic fields in density functional theory, *J. Chem. Theory Comput.* **14**, 1247 (2018).
- [37] D. J. Singh, *Planewaves Pseudopotentials and the LAPW Method* (Kluwer Academic Publishers, Boston, 1994).
- [38] J. K. Dewhurst and S. Sharma *et al.*, (Jan. 14 2018) <http://elk.sourceforge.net/>.
- [39] J. E. Peralta, O. Hod, and G. E. Scuseria, Magnetization dynamics from time-dependent noncollinear spin density functional theory calculations, *J. Chem. Theory. Comput.* **11**, 3661 (2015).
- [40] J. K. Dewhurst, K. Krieger, S. Sharma, and E. K. U. Gross, An efficient algorithm for time propagation as applied to linearized augmented plane wave method, *Comput. Phys. Commun.* **209**, 92 (2016).
- [41] F. Willems, C. T. L. Smeenk, N. Zhavoronkov, O. Kornilov, I. Radu, M. Schmidbauer, M. Hanke, C. v. K. Schmising, M. J. J. Vrakking, and S. Eisebitt, Probing ultrafast spin dynamics with high-harmonic magnetic circular dichroism spectroscopy, *Phys. Rev. B* **92**, 220405 (2015).
- [42] B. Koopmans, G. Malinowski, F. Dalla Longa, D. Steiauf, M. Fahnle, T. Roth, M. Cinchetti, and M. Aeschlimann, Explaining the paradoxical diversity of ultrafast laser-induced demagnetization, *Nat. Mater.* **9**, 259 (2010).
- [43] B. Koopmans, H. H. J. E. Kicken, M. van Kampen, and W. J. M. de Jonge, Microscopic model for femtosecond magnetization dynamics, *J. Magn. Magn. Mater.* **286**, 271 (2005).
- [44] B. Koopmans, J. Ruigrok, F. Dalla Longa, and W. de Jonge, Unifying Ultrafast Magnetization Dynamics, *Phys. Rev. Lett.* **95**, 267207 (2005).
- [45] A. Melnikov, I. Razdolski, T. O. Wehling, E. T. Papaioannou, V. Roddatis, P. Fumagalli, O. Aktsipetrov, A. I. Lichtenstein, and U. Bovensiepen, Ultrafast Transport of Laser-Excited Spin-Polarized Carriers in Au/Fe/MgO(001), *Phys. Rev. Lett.* **107**, 076601 (2011).
- [46] J. K. Dewhurst, P. Elliott, S. Shallcross, E. K. U. Gross, and S. Sharma, Laser-induced intersite spin transfer, *Nano Lett.* **18**, 1842 (2018).
- [47] P. Elliott, T. Mueller, J. K. Dewhurst, S. Sharma, and E. K. U. Gross, Ultrafast laser induced local magnetization dynamics in Heusler compounds, *Sci. Rep.* **6**, 38911 (2016).
- [48] J. Chen, U. Bovensiepen, A. Eschenlohr, T. Mueller, P. Elliott, E. K. U. Gross, J. K. Dewhurst, and S. Sharma, Competing spin transfer and dissipation at Co/Cu(001) interfaces on femtosecond timescales (2018).
- [49] N. Moisan, G. Malinowski, J. Mauchain, M. Hehn, B. Vodungbo, J. Lüning, S. Mangin, E. E. Fullerton, and A. Thiaville, Investigating the role of superdiffusive currents in laser induced demagnetization of ferromagnets with nanoscale magnetic domains, *Sci. Rep.* **4**, 4658 (2014).
- [50] A. J. Schellekens, W. Verhoeven, T. N. Vader, and B. Koopmans, Investigating the contribution of superdiffusive transport to ultrafast demagnetization of ferromagnetic thin films, *Appl. Phys. Lett.* **102**, 252408 (2013).
- [51] M. Battiato, K. Carva, and P. M. Oppeneer, Superdiffusive Spin Transport as a Mechanism of Ultrafast Demagnetization, *Phys. Rev. Lett.* **105**, 027203 (2010).